VIROLOGY

Periodic shifts in viral load increase risk of Hendra virus spillover from *Pteropus* bats

Tamika J. Lunn[1,2], Benny Borremans[3,4], Devin N. Jones-Slobodian[5], Maureen K. Kessler[6], Adrienne S. Dale[7], Claude K. Yinda[8], Manuel Ruiz-Aravena[9], Caylee A. Falvo[10], Daniel E. Crowley[10], James O. Lloyd-Smith[11], Vincent J. Munster[8], Peggy Eby[12,13], Hamish McCallum[12], Peter Hudson[14], Olivier Restif[15], Liam P. McGuire[16], Ina L. Smith[17], Bat One Health Group Collaborators†, Raina K. Plowright[10]*‡, Alison J. Peel[12,18,19]*‡

Prediction and management of zoonotic spillover requires an understanding of infection dynamics within reservoir host populations. Spillover risk is commonly inferred from infection prevalence based on detection of viral genomic material, yet detection alone does not indicate the presence of infectious virus or a sufficient dose for transmission. We undertook a comprehensive investigation of Hendra virus shedding in its primary reservoir, *Pteropus* bats, analyzing quantitative PCR with reverse transcription (RT–qPCR) data from 6151 pooled urine samples collected across five sites over 3 years. We assessed longitudinal associations between viral prevalence (proportion of positive pooled urine samples), viral load proxies, and equine spillover, using generalized additive models and a permutation analysis. Peak prevalence periods associated with spillover events ($N = 5$) had a higher proportion of samples with high viral loads than periods without spillover. Prolonged periods of low viral load and low prevalence likely reflect noninfectious RNA or doses insufficient for cross-species transmission. Incorporating viral load metrics alongside prevalence can improve prediction of spillover risk.

INTRODUCTION

Spillover of zoonotic infections with epidemic potential is a public health concern. A major challenge for the design and implementation of preemptive strategies emerges from the complex, multilayered nature of cross-species transmission (*1*). The pathogen, its reservoir host(s), environment, and potential novel hosts are connected dynamically in space and time, with intermittent opportunities for cross-species transmission when conditions align. The dynamics of pathogen circulation in reservoir host populations are an important determinant of spillover risk and are usually assessed through the prevalence of infection in space and time. Although viral load is considered crucial, it is rarely included in empirical spillover studies (*2*).

Estimation of prevalence based on binary detection/nondetection of genomic material—without accounting for biological processes (*3*–*5*)—may decouple pathogen presence from infectiousness, and thereby risk of transmission (*6*). Viral shedding can be noninfectious in two key ways: Either the shed viral load is too low to overcome dose barriers, or the shed virus itself is no longer capable of causing infection. In the latter case, the immune response may neutralize the virus without eliminating degraded nucleic/ribonucleic acid (*6*). For example, lysed or aggregated viral particles may be shed as nonenveloped, relatively stable nucleoprotein complexes, lacking active infection or the production of infectious virions (*7*). Because assays target specific RNA segments, even extensive immune-mediated degradation may have minimal impact on RNA detection. Diagnostic assays typically use thresholds designed to maximize detection sensitivity [e.g., a cycle threshold (Ct) value of 40 is traditionally used for quantitative polymerase chain reaction assays]. However, such thresholds may not distinguish between infectious virus and residual or degraded viral RNA, which complicates efforts to assess and predict infectious virus excretion and the potential for spillover.

Viral load in humans has been used to estimate transmissibility (e.g., HIV) (*8*) and to predict patient outcome (e.g., Ebola virus disease) (*9*). Recent research prompted by the COVID-19 pandemic has further demonstrated the utility of viral load proxies in predicting trajectories of epidemics in epidemiological modeling (*10*). Integrating viral load proxies with prevalence in wildlife epidemiological studies may better represent infected versus infectious states, virus distribution across landscapes, and the doses available for recipient hosts (*1*). Quantitative measurement of viral shedding intensity—particularly using genome copy numbers as a proxy of viral load—is a valuable but underexplored addition to models predicting spillover risk from wildlife.

Hendra virus is a bat-borne paramyxovirus (genus: *Henipavirus*) that causes severe disease and death in horses and humans in eastern

[1]Odum School of Ecology, University of Georgia, Athens, GA 30602, USA. [2]Center for the Ecology of Infectious Diseases, University of Georgia, Athens, GA 30602, USA. [3]Wildlife Health Ecology Research Organization, San Diego, CA 92107, USA. [4]Evolutionary Ecology Group, University of Antwerp, Antwerp, Belgium. [5]Department of Microbiology and Cell Biology, Montana State University, Bozeman, MT 59715, USA. [6]Department of Ecology, Montana State University, Bozeman, MT 59715, USA. [7]Department of Biological Sciences, Texas Tech University, Lubbock, TX 79409, USA. [8]Laboratory of Virology, National Institute of Allergy and Infectious Diseases, National Institutes of Health, Hamilton, MT 59840, USA. [9]Department of Wildlife, Fisheries and Aquaculture, Mississippi State University, Starkville, MS 39759, USA. [10]Department of Public and Ecosystem Health, College of Veterinary Medicine, Cornell University, Ithaca, NY 14853, USA. [11]Department of Ecology and Evolutionary Biology, University of California Los Angeles, Los Angeles, CA 90095, USA. [12]Centre for Planetary Health and Food Security, Griffith University, Nathan, QLD 4111, Australia. [13]School of Biological Earth and Environmental Sciences, University of New South Wales, Sydney, NSW 1466, Australia. [14]Center for Infectious Disease Dynamics, Pennsylvania State University, State College, PA 16801, USA. [15]Department of Veterinary Medicine, University of Cambridge, Cambridge CB3 0ES, UK. [16]Department of Biology, University of Waterloo, Waterloo, ON N2L 3G1, Canada. [17]Health and Biosecurity Business Unit, Commonwealth Scientific and Industrial Research Organisation (CSIRO), Canberra, ACT 2601, Australia. [18]Sydney School of Veterinary Science, University of Sydney, Sydney, NSW 2006, Australia. [19]Sydney Infectious Disease Institute (Sydney ID), Faculty of Medicine and Health, University of Sydney, Sydney, NSW 2006, Australia.
*Corresponding author. Email: alison.peel@sydney.edu.au (A.J.P.); rkp57@cornell.edu (R.K.P.)
†Bat One Health Group collaborators and affiliations are listed in the Supplementary Materials.
‡These authors contributed equally to this work.

Australia (*11*). Equine cases have been reported annually with clusters in some years (*12*). A total of 68 spillover events, involving 110 confirmed or suspected cases in horses, and 7 confirmed human cases, have been reported since the virus was first detected in 1994, including two detections of a recently found variant (HeV-g2) in horses (*12*, *13*). Because of high virulence and recurrent spillover, the World Health Organization has classified henipaviruses as "high priority" for future research (*14*).

Despite the alignment of flying-foxes and horses across most of eastern Australia, spillovers have only been detected in coastal New South Wales and Queensland (fig. S1). Most occur in winter in the subtropics and in clusters that occur with interannual variation (*12*). In part, this may be explained by increased prevalence in bats (as measured by the proportion positive for Hendra virus shedding) in winter, and the varying magnitude and timing of shedding prevalence (*15*, *16*). Previous work also suggests periods of low off-season prevalence in roosts from subtropical Australia and consistent low-prevalence shedding from roosts in tropical Australia (*15*, *17*). Why these prolonged periods of shedding do not translate to spillover has been a persistent puzzle. It is also unclear whether cumulative, low-level shedding over a long time presents a similar risk as high-level shedding over a short time (*17*). We hypothesize that incorporating viral load proxies into longitudinal studies of virus excretion will improve predictions of periods and places of high spillover risk.

We tested whether temporal variation in viral load is more predictive of spillover risk than prevalence alone. We sampled five flying-fox roost sites in subtropical Australia for 3 $^{1}/_{2}$ years (Fig. 1), and screened for excretion of Hendra virus (HeV-g1). We incorporated viral load proxies (Ct and genome copy numbers) to estimate the amount of infectious virus shed, and used a permutation analysis to test whether Ct values were nonrandomly distributed over time. We focused on roosts with ecological characteristics linked to high risk of spillover (*12*, *16*) (Table 1) and used an optimized pooled sampling method (*18*) to improve the accuracy of prevalence estimates. Together, this dataset and multifaceted analyses provide insights into observed but unexplained patterns of shedding and spillover and will contribute to the future management of viral spillover risk.

RESULTS

We tested 6151 unique pooled urine samples from 152 sampling sessions collected from July 2017 through September 2020 for the presence of prototypic Hendra virus (HeV-g1), the variant responsible for 97% (66 of 68) of known spillover events. For 4657 of these samples, at least one black flying-fox was recorded above the collection sheet, with a median of three flying-foxes above each sheet per session. Herein, we use the latter subset of 4657 samples, as black flying-foxes are the primary reservoir for the prototypic Hendra virus variant tested. Using the conventional Ct 40 threshold, 361 of 4657 samples were positive for Hendra virus (8%) with a mean viral load of 22,000 genome copies/ml. For the samples with available data, the GPS–estimated distance between sheets was a median of 2 to 10 m.

We observed seasonal and interannual patterns in shedding prevalence. To facilitate comparison across Ct thresholds, we calculated the normalized pooled prevalence as the proportion of samples testing positive, normalized by the maximum prevalence across the dataset for each threshold. With high Ct threshold values, viral excretion typically peaked in the winter season (Jun to Aug), but low-prevalence

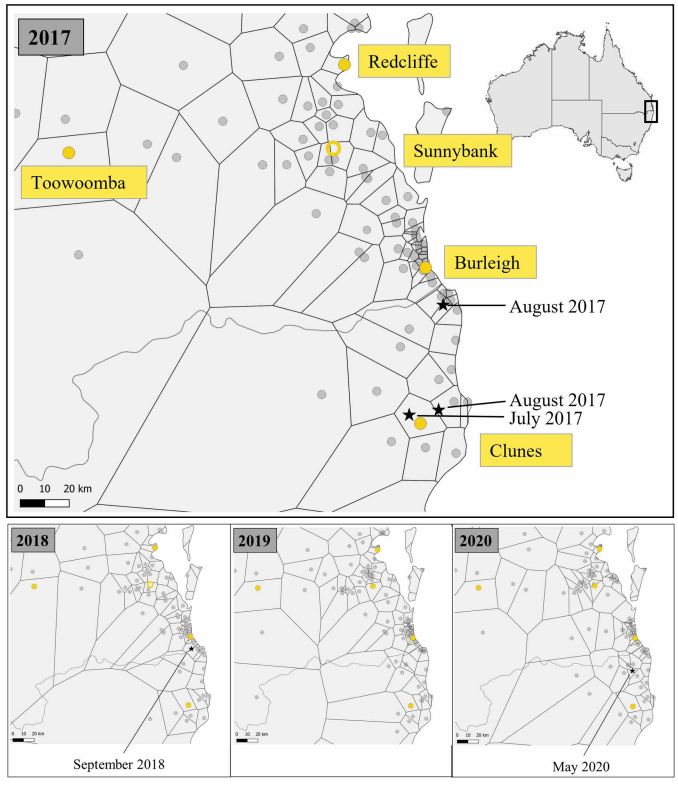

Fig. 1. Location of winter-occupied flying-fox roosts (gray circles) and Hendra virus spillover events (black stars) in the study area, per study year (2017–2020). Tessellation boundaries show the nearest winter-occupied flying-fox roost for any given location. Roosts sampled for the present study are shown in yellow. Note that the roost site "Sunnybank" was not occupied over winter in 2017. The location of the roost is shown as a hollow circle on the 2017 and 2018 panels for reference. Flying-fox roost locations obtained from Eby *et al.* (*12*).

shedding was apparent throughout the rest of the year. Using lower Ct thresholds, pooled prevalence was minimal outside of winter. Large peaks in prevalence were not observed every year, and this was consistent across all thresholds (Fig. 2).

We undertook a permutation analysis to test whether viral load and prevalence were associated (i.e., whether Ct values were nonrandomly distributed) over time. For this, Ct values from positive samples (Ct $\leq$ 40) were randomly shuffled across sessions, so that prevalence at the Ct $\leq$ 40 threshold within any given sampling session was preserved but the Ct value of positive samples within that session was randomized. Prevalence was then reestimated as increasingly conservative Ct thresholds were reapplied. Across conservative thresholds, divergence between observed and permuted normalized prevalence curves identifies periods when the observed data contain more or fewer positives than expected under a random distribution of viral loads, indicating shifts in shed viral loads.

The permutation analysis of normalized pooled prevalence showed strong support for a Ct distribution shift toward disproportionately lower values (higher viral loads) during high-prevalence periods, and toward disproportionately higher values (lower viral loads) during low-prevalence periods (Fig. 2), as shown by divergence between observed and permuted prevalence curves. Across Ct thresholds, high quantiles coincided with high-prevalence periods (i.e., observed prevalence being higher than most permuted prevalence values) and low

Table 1. Ecological and feasibility criteria for roost selection.

Category	Criterion
Ecological characteristics associated with spillover risk (*12*, *16*)	Continuous occupation by black flying-foxes (*Pteropus alecto*; the primary reservoir for the prototypic Hendra virus variant HeV-g1)
	Recently established as overwintering roost
	Highly restricted access to native winter food sources
Feasibility	Roost population consistently large enough for sufficient sample sizes ($N > 500$)
	Suitable access and sampling conditions
	Not a site of high human-bat conflict
	Long-term sampling permissions obtainable

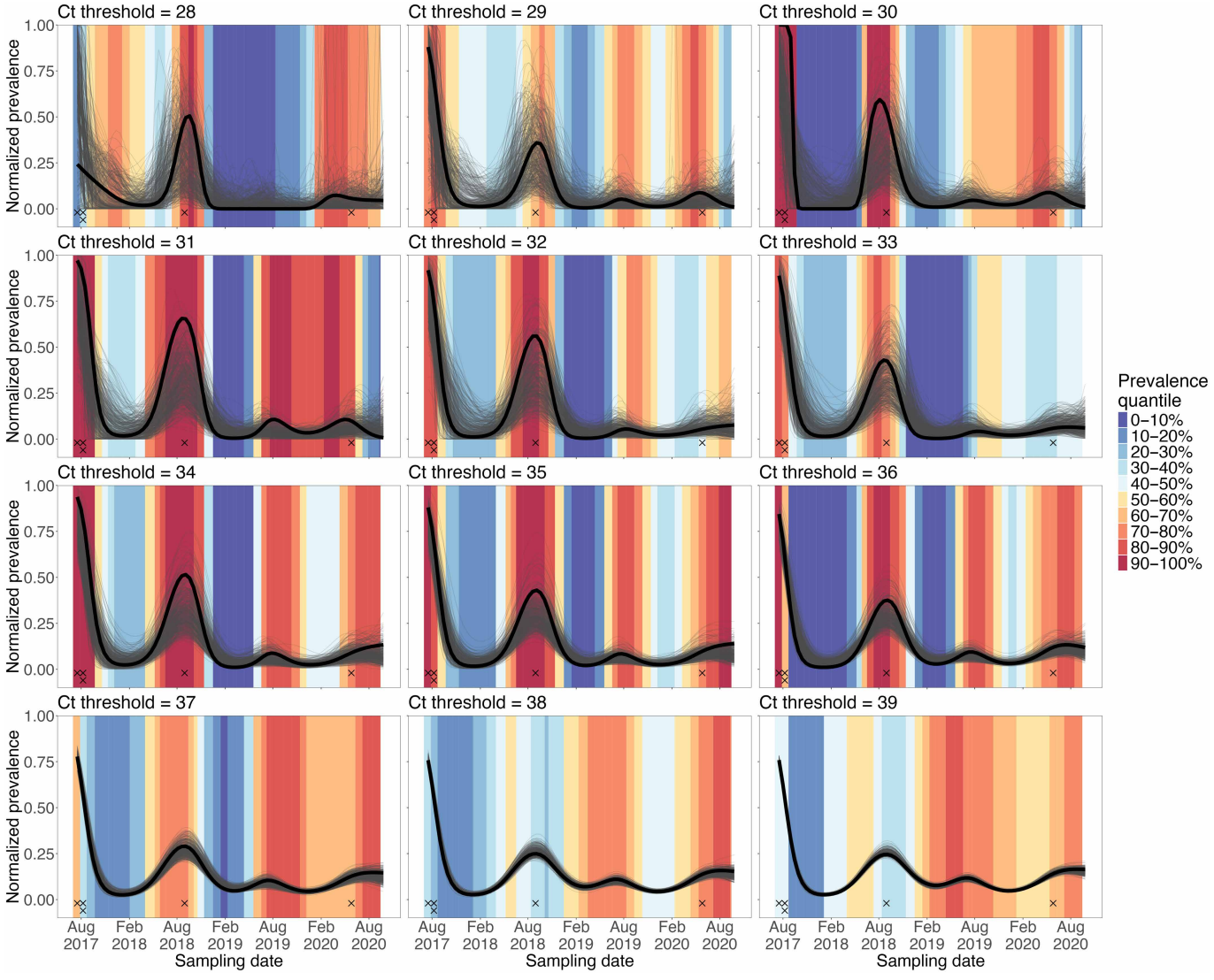

Fig. 2. Permutation analysis at different Ct thresholds. Ct values for all samples (Ct ≤ 40) were permuted 500 times, and prevalence was reestimated using a new Ct threshold (Ct < 40). Permuted curves are shown as thin gray lines, and observed prevalence is shown as a bold black line. For each time point, the quantile of observed prevalence was calculated as the proportion of permuted prevalence values that was smaller than the observed value, and these quantiles are visualized using the background colors. When Ct distributions are similar over time, prevalence quantiles are expected to be around 50%, whereas changing Ct distributions are expected to result in low and high quantiles. Prevalence is pooled for all sites and normalized to allow comparison between thresholds. Note that points in the normalized time series reach one, but that the prevalence curves are smoothed, meaning they do not necessarily pass through one. Cases of spillover are shown with crosses.

quantiles coincided with low-prevalence periods, but only for thresholds below Ct 38.

Cases of spillover aligned with peaks in normalized pooled prevalence estimated using lower Ct threshold values (Fig. 2). When the time series was subdivided based on season and spillover, normalized prevalence was highest for peak seasons in which a spillover event was observed, and this was consistent for all Ct threshold values (Fig. 3) (effect size ± SE: peak season and spillover = 13.7 ± 1.43, peak season and no spillover = 2.33 ± 1.34, $P < 0.0001$, df = 2, $\chi^2 = 53.2$). For peak season with spillover events, normalized prevalence trended higher for lower Ct threshold values, excluding the two lowest values where sample sizes of positives were very small (e.g., 16 positive samples at Ct 28, and 26 at Ct 29, compared with 160 at Ct 35) (Fig. 3). However, this trend was not statistically supported (effect size = 0.90, $P = 0.30$, df = 1, $\chi^2 = 1.12$). These results were further supported by the permutation analysis, as the association between normalized pooled prevalence and spillover was stronger for threshold values below Ct 38. This was shown by the low Akaike information criterion (AIC) quantiles for generalized linear models (GLMs) linking normalized pooled prevalence to number of spillover events and, to a lesser degree, for GLMs linking normalized pooled prevalence to occurrence of spillover events (Fig. 4). Results were consistent when repeated using the Clunes-only dataset (Supplementary Materials; figs. S17 and S18). Note that these models are not intended for formal (absolute) inference due to limited statistical power. Instead, they offer a consistent comparative framework for evaluating how changes in prevalence, under different Ct thresholds, relate to spillover risk.

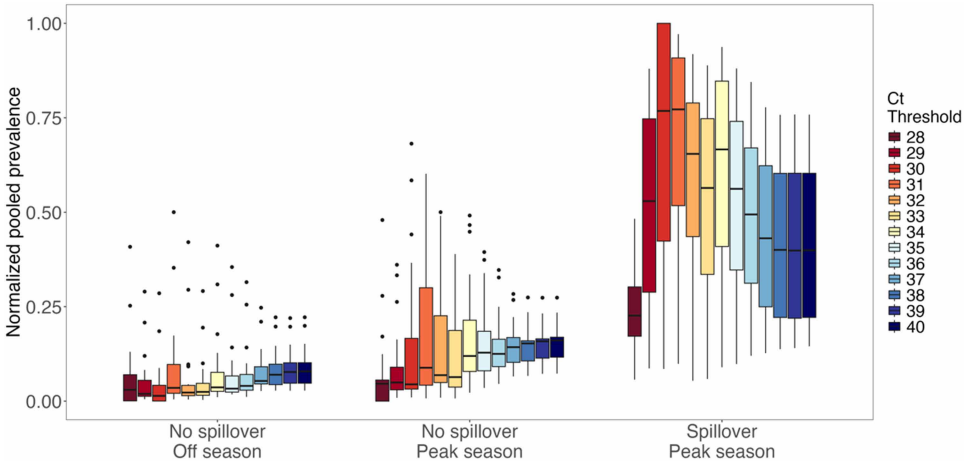

Fig. 3. Normalized pooled prevalence for different Ct threshold values across off-season months (September to May) with no cases of spillover, and peak season (June to August) without and with cases of spillover. Boxplots show the 25th, 50th, and 75th percentiles, lines indicate the smallest and largest values within 1.5 times the interquartile range, and dots indicate values beyond that. Normalization is intended to show the relative changes in prevalence across the time series (therefore, how the dynamics of prevalence vary), for each Ct threshold. If prevalence is predictive of spillover, there will be relatively low prevalence values in months with no spillover, and relatively high prevalence values in months with spillover (as seen). If different thresholds are more or less predictive of spillover, there will be a systematic trend in relative prevalence values across the Ct threshold values, such that there will be more differentiation between prevalence estimated using more conservative Ct values, between the no-spillover and spillover months (also as seen; i.e., prevalence values trend lower for months with no spillover, and higher in months with spillover, for increasingly conservative Ct values).

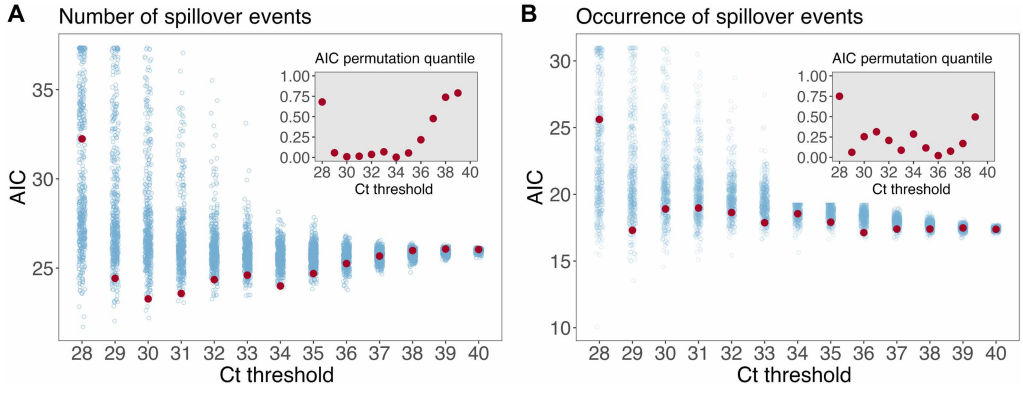

Fig. 4. Akaike information criterion (AIC) values for models with normalized pooled prevalence as the predictor variable and either number or occurrence of spillover events as the outcome variable, for a range of Ct thresholds. (**A** and **B**) show results for spillover number and spillover occurrence, respectively. AIC values are shown in blue for permuted data and red for observed data. Insets show the proportion of permuted AIC values that is larger than the observed value. Low quantile values provide statistical support for a shift in the distribution of Ct values that results in a better correlation between prevalence and spillover. Note that while AIC values for the lowest Ct thresholds are shown for consistency, they are not reliable due to the very low number of positive samples remaining after applying the most stringent thresholds.

DISCUSSION

We demonstrate periodic shifts in the viral load shed by *Pteropus* bat populations, skewing toward higher viral loads of Hendra virus during high-prevalence periods. These results support the hypothesis that spillover risk increases disproportionately when both prevalence and individual viral loads are elevated. While our sampling resolution was insufficient to determine the fine scale temporal sequencing of these events, prior modeling studies in humans [e.g., (*10*)] predict that viral load peaks before prevalence. In addition, using more conservative Ct thresholds generated prevalence estimates that more strongly correlated with spillover risk. Collectively, these findings suggest that conventional detection of Hendra virus RNA at Ct 40 may not be the best threshold for predicting spillover.

The Hendra virus RT-PCR (TaqMan) assay was developed to diagnose Hendra virus infection specifically and rapidly, to allow prompt implementation of control measures on infected properties (*19*). The priority—to identify infected but not necessarily infectious animals—balances the need for a high detection rate with a small proportion of false positive results (*19*). In clinical settings where the consequences of a missed assessment are great, a high probability of detection with few misses is appropriate. Detection of Hendra virus RNA for exclusion testing uses a Ct 40 threshold for this reason (*15*). Wildlife epidemiological studies, by contrast, preemptively identify spatiotemporal patterns of risk to inform future management. Modeling tools often assume that RNA detection equates to infectiousness (susceptible, infectious, recovered models) (*20*). In these scenarios, identification of hosts that are actively infectious is an appropriate priority. Though the precise functional relationship between infectivity and viral load is currently unknown for even the most well-studied viruses (e.g., SARS-CoV-2), it is widely accepted that individuals with higher viral loads are more likely to be infectious (*10*, *21*, *22*).

Using lower Ct thresholds, pooled prevalence was minimal outside of peak season, and large peaks of infectiousness were not observed every year. In addition, normalized pooled prevalence estimated using lower Ct thresholds was higher than the conventional estimate during peak seasons where spillover events were observed, but lower during peak seasons where no spillover events were observed, or during the off season. Collectively, these results suggest that prolonged low-intensity shedding of Hendra virus outside of winter months—detected only when using the conventional threshold—may reflect either prolonged shedding of noninfectious RNA or viral loads too low to overcome dose barriers to spillover infection. In other words, while these low viral loads may contribute to transmission and maintenance of Hendra virus within the natural bat reservoir host, they appear to pose minimal risk for cross-species transmission. More broadly, this observation may reflect a general pattern among Hendra virus variants. Specifically, the comparatively lower prevalence and viral loads reported for Hendra virus genotype 2 in wild flying-fox populations, relative to genotype 1, may partially contribute to a lower spillover risk for this variant. However, this pattern should be interpreted with caution until large-scale surveillance of both genotypes is undertaken simultaneously, under the same conditions (*23*).

Various mechanisms have been proposed to explain patterns in Hendra virus infection in subtropical Australia, including the temporal availability of eucalyptus blossom—the preferred food of flying-foxes (*12*, *24*). Low food availability and utilization of alternative diet sources may lead to increased viral shedding via reduced immunocompetence and reactivated infection (*16*, *25*), a mechanism demonstrated in experimental systems of other bat pathogens (*26*). In winter, few species of eucalyptus reliably produce nectar (*27*); this period of food scarcity coincides with the higher levels of Hendra virus shedding in subtropical regions reported here and elsewhere (*15*, *17*). This mechanism may also explain the stronger predictive power of models that used number of spillovers rather than occurrence (Fig. 4). While Hendra virus circulates endemically within *Pteropus* bat populations, clusters of spillover events (≥3 events) follow severe climate-driven food shortages that are not mitigated by subsequent winter flowering pulses. Outside of these conditions, spillovers occur as isolated events in most years (*12*). This highlights the potential role of nutritional stress in periods of elevated risk. Further analyses will be required to assess whether food availability and nutritional composition explains the distributional shifts in viral load, and the link to spillover frequency, as shown here.

Note that our study intentionally focused on roosts with highly restricted access to native winter food sources, as this attribute is linked to spillover, and that replication of roosts was limited (five roosts). Observed patterns of actual prevalence values and dynamics may not be generalizable to roosts that do not experience acute food shortages, and will not be generalizable over space and through time. However, we do expect the interplay between prevalence and Ct cutoffs to be generalizable across roosts, as this was observed consistently over time. We observed consistent patterns over time for the five roosts, including when the data were analyzed as an aggregate of the five roosts, or as the singular roost that was spatially linked with spillover events. This suggests that there are predictable periods when a higher proportion of individuals shed large viral loads, and vice versa, which can be detected using different Ct thresholds.

To further explore the relationship between viral load proxies and infectiousness, future studies could formally test a serial dilution relationship between RNA detection (genome copy numbers) and in vitro infectiousness [median tissue culture infectious dose ($TCID_{50}$)] of henipaviruses on different cell lines, or in vivo infectiousness (infectious dose) for nonhuman primate or small animal models (*5*, *28*). As this relationship becomes clearer, future models of bat-pathogen transmission dynamics may also consider RNA shedding along with antibody responses to incorporate within-host infection dynamics into spillover risk estimates.

Our exploration of alternate Ct thresholds is intended to emphasize detections relevant for transmission—i.e., higher viral loads that are more likely to be functionally infectious (*10*, *21*, *22*). We would note that multiple factors contribute to whether a single Ct value or viral load detected within an individual ultimately results in transmission and, therefore, that there is no perfect threshold for infectivity. While lower Ct thresholds generally improved the association between prevalence and spillover, we found no specific optimal value or a clear trend toward stronger correlations for lower values. While more conservative thresholds are more likely to represent infectious virus, we acknowledge that infectious virus could also be possible above a given threshold. The intention of our approach is to explore whether different thresholds alter the observed viral dynamics in ways that are meaningful for interpretation of viral transmission dynamics and spillover, rather than find an optimal Ct value for use in Hendra virus epidemiology. Future studies that seek to compare Ct values with results in this study should also consider that Ct values alone are not directly comparable across laboratories (*28*).

In addition, although we took steps to estimate true prevalence from pooled samples, we acknowledge potential error in overhead counts, and cannot fully exclude bat movement among sheets or

overestimation from a "superspreader." However, counting errors are expected to be minimal (see Supplementary Text) with limited impact on prevalence as per sensitivity analyses in Borremans *et al.* (*29*). Bat movement is likewise expected to be minimal (see Supplementary Text) with any movement likely only to create random noise, rather than systematic bias in prevalence estimates. Consequently, we consider these factors unlikely to affect interpretations as presented.

In conclusion, we challenge the current paradigm that higher prevalence of viral shedding in reservoir hosts is a lone driver of spillover from wildlife to humans. We show that there is a temporal shift in the distribution of Hendra virus load proxies in *Pteropus* bat populations and that accounting for viral load generates prevalence estimates that more strongly correlate with observed Hendra virus spillovers. We suggest that estimates of prevalence that ignore declining viral load can decouple the presence of virus from the risk of transmission, and that previously reported low-prevalence shedding of Hendra virus does not align with spillover risk. Our study provides a key insight into the processes that facilitate spillover and offers a foundation for further investigations in other systems and experimental studies to explore the mechanisms driving high viral shedding in bats, as well as their potential generalizability across species, regions, and viruses. Obtaining data to refine Ct thresholds that more accurately indicate infectiousness remains a priority for advancing this field.

MATERIALS AND METHODS

We conducted our study from July 2017 through September 2020 at five roosts spanning southeast Queensland to northeast New South Wales ("Redcliffe," "Sunnybank," "Toowoomba," "Burleigh," and "Clunes"; Fig. 1). Roosts were selected for attributes associated with spillover (*12*, *16*) and feasibility (Table 1).

The commencement of sampling was staggered across sites, with all sites incorporated by April 2018. Roosts were sampled approximately monthly, with most sampled within the same week each month. Analyses were performed on approximately monthly sampling sessions from aggregated roost sites, with clusters of sessions defined so that all sessions within each cluster occurred within 14 days of one another. Given the high mobility of black flying-foxes (*30*), and that all study roosts share ecological characteristics and similar latitudes within a subtropical climate zone (~170 km north to south), we assume that individuals mix among roosts experiencing broadly comparable conditions. This supports the aggregation of data for the analyses. Five Hendra virus equine spillover events occurred in the study area during our sampling period, with two falling within the foraging radius of our study sites (a single study site, Clunes) (*12*).

Sample collection

At each site, we collected pooled urine samples from beneath roosts using plastic sheets (0.9 × 1.3 m) distributed before sunrise (~4 a.m. to 6 a.m. AEST), following an optimized sampling approach (Supplementary Text). Sheet placement (and downstream analyses) targeted black flying-foxes (*Pteropus alecto*), but gray-headed (*Pteropus poliocephalus*) and, rarely, little red flying foxes (*Pteropus scapulatus*) were also sampled. Sample collection began once bats had returned to the roost and concluded within 6 hours. The number and species of individuals roosting over the sheet were recorded. We pooled urine on each sheet into a single sample (roughly 20 urine droplets to a volume of ~2 ml), and aliquoted up to three cryovials for Hendra virus testing containing AVL buffer (Qiagen) (target 140 µl of urine into 560 µl of buffer), viral transport medium (VTM) (*28*) (between 200 and 1000 µl of urine into 1000 µl of VTM), and no buffer (NB). Samples were transported in a CryoShipper (<−80°C) and stored at −80°C. An average of 40 pooled samples were collected per session. Urine was not collected from sheets if the urine had completely evaporated or was contaminated with feces (~0.7% of samples). Rain-affected sampling events were abandoned and rescheduled.

Screening of Hendra virus using quantitative PCR with reverse transcription (RT–qPCR)

We used the QIAamp Viral RNA Kit and QIAcube HT automated system (Qiagen) to extract RNA. RNA was eluted in 150 µl of TE buffer. A Hendra virus genotype 1 (HeV-g1) duplex RT–qPCR assay was used for the detection of viral RNA (targeting the *P* gene, primer, and probe sets given in the Supplementary Materials; table S2). This assay specifically targets HeV-g1 and does not detect HeV-g2 (*23*). In the RT–qPCR, 10 µl of RNA and 900 nM and 250 nM final concentrations of primer and probe, respectively, were tested with 10 µl of TaqMan Fast Virus 1-Step master mix on a QuantStudio 6 flex Real-Time PCR instrument (Applied Biosystems). Thermocycling conditions are given in the Supplementary Materials (table S3). Positive standards (with known genome copy numbers previously quantified using droplet digital PCR) were run in parallel with samples at 10-fold dilutions to construct a standard curve and calculate genome copy numbers per milliliter of each positive sample (Supplementary Materials; table S4).

Higher viral loads are more likely to be functionally infectious (*10*, *21*, *22*). We considered genome copies and Ct values from pooled samples to be proxies for the viral load available to recipient spillover hosts, as is common practice in epidemiological studies (*10*, *21*, *22*). We use the term "viral load" throughout to refer to these proxies, though we note that the term "viral load" is used beyond the historical virological definition [which only uses $TCID_{50}$ or plaque-forming units (PFU) to describe viral load]. Note that the Ct value is the number of cycles needed to amplify enough target nucleic acid to be detected. Thus, Ct values are inverse to the amount of target nucleic acid in a sample; a lower Ct value corresponds to more target nucleic acid (higher viral load). Traditionally, amplification within 40 cycles is used to declare a sample positive. However, it is important to note that the exact threshold is set during assay validation and reflects both practical limits and the primary objectives of the assay (for example, avoiding false-negative results in diagnostics).

Statistical analysis

We analyzed pooled urine samples with at least one (but not exclusively) black flying-fox recorded above the sheet (4657 of 6151 samples, 75.7%). We assessed whether viral loads were randomly distributed relative to time and prevalence, or whether there were periods during which the proportion of individuals shedding high loads was larger, using a permutation analysis. First, we estimated a proxy for prevalence as the proportion of pooled urine samples positive for Hendra virus (with Ct ≤ 40), with temporal dynamics estimated from a generalized additive model fitted to time. Models used a binomial distribution with a logit-link, with prevalence modeled as a natural cubic spline with 8 degrees of freedom. Model fits were repeated for different Ct thresholds that determine sample positivity, ranging from Ct 28 (~100,000 genome copies/ml) to Ct 39 (~100

genome copies/ml). Ct 40 is not reported because the permuted prevalence dynamics at this threshold are identical to those observed in the original data (see explanation of the permutation process below). To allow comparison between Ct threshold values, prevalence was normalized by dividing by maximum prevalence across the dataset for each threshold. Normalized prevalence should be interpreted as a relative value, where high values indicate when prevalence is high relative to other values in the time series for each Ct threshold. For nonnormalized prevalence values at each Ct threshold, see the Supplementary Materials (figs. S12 to S15).

Permutations randomly shuffled Ct values of positive samples (with positivity determined using the "baseline" Ct threshold of 40) to reestimate normalized pooled prevalence dynamics with randomized time. Ct thresholds were applied after each permutation procedure, meaning that after the random shuffling step, all samples with a Ct value larger than the threshold value were considered negative. The observed and permuted prevalence curves would remain similar if Ct values were randomly distributed over time, or random relative to normalized prevalence, because the proportion of samples that remain positive would be similar regardless of the time point, or whether normalized prevalence was high or low (i.e., the observed values and permuted values are both random). If Ct values were nonrandomly distributed, then the observed and permuted prevalence curves would diverge when values are randomized by the permutation. This is because the observed data at particular times would contain relatively more, or relatively fewer, positive samples than the (randomized) permuted data, which would present as relatively higher peaks and lower troughs in the observed prevalence curve relative to the permuted curves. Divergence between curves should become more apparent with more conservative Ct thresholds, as relatively more or fewer samples are retained as "positive" at those time points when the underlying distribution of viral loads is skewed. Permuted prevalence dynamics estimated using the conventional Ct threshold (Ct 40) would be the same as for the observed data, as all samples are retained as positive.

During the permutation process, we explicitly accounted for the fact that the viral load of a pooled sample is the result of contributions from both positive and negative bats, where the number of positive bats is unknown, as per Borremans *et al.* (*29*). We ensured our results were robust to uncertainty in the number of positive bats contributing to a pooled sample and interindividual variation in viral loads using simulated data and permutation tests (see Supplementary Materials; fig. S2). The permutation process also accounts for potential differences in preservative type (AVL, VTM, or NB), by restricting shuffling to samples within the same preservative type. Further, we used simulation tests to confirm our analyses with the empirical data we collected were sufficient to detect changes in viral load when that load varies with viral prevalence (see Supplementary Materials; fig. S3).

We compared normalized pooled prevalence dynamics estimated using original Ct values with 500 permuted prevalence curves. For this, we calculated the proportion of permuted prevalence values that were smaller than the observed prevalence value at each time point (i.e., the observed prevalence quantile). If there was no change in the distribution of Ct values over time, the quantiles would be relatively constant around ~50%. If Ct values shifted toward low values (high viral loads; e.g., during high-prevalence periods) and vice versa, the quantiles would be high during high-prevalence periods and low during low-prevalence periods.

To visualize whether lower Ct thresholds improved the association between normalized pooled prevalence and spillover risk, we divided the time series by off-season months (i.e., those with seasonally low prevalence; September to May) (*12*) with no cases of spillover, and peak-season months (i.e., those with seasonally high prevalence; June to August) with and without cases of spillover (giving three time-series categories), and plotted the normalized pooled prevalence estimated for each Ct threshold. We fitted GLMs (binomial error distribution and logit link function) to test the correlation between (i) monthly normalized pooled prevalence and time-series category across Ct values, and (ii) monthly normalized pooled prevalence and Ct threshold value during peak season with spillover only.

To test whether lower Ct thresholds improved the association between normalized pooled prevalence and spillover risk, we also fitted a GLM to the number of spillover events (Poisson error distribution and log link function) and the occurrence of spillover events (binomial error distribution and logit link function), repeated for each Ct threshold. Predictor variables were either the monthly observed or the monthly permuted (normalized) pooled prevalence estimates. A measure of model fit (AIC) was then used to assess (i) whether model fit improved for lower thresholds, and (ii) whether model fit improved relative to the permuted datasets. Analyses including spillover data were performed on sites aggregated across space, and for the single study site (Clunes) spatially linked with spillovers during the duration of the study (Supplementary Materials; fig. S16). All analyses were undertaken in R version 4.2.2 using the "stats" (v4.2.2) package (*31*).

Supplementary Materials

This PDF file includes:

Supplementary Text
Figs. S1 to S18
Tables S1 to S4
References

REFERENCES

1. R. K. Plowright, C. R. Parrish, H. McCallum, P. J. Hudson, A. I. Ko, A. L. Graham, J. O. Lloyd-Smith, Pathways to zoonotic spillover. *Nat. Rev. Microbiol.* **15**, 502–510 (2017).
2. T. J. Lunn, O. Restif, A. J. Peel, V. J. Munster, E. De Wit, S. Sokolow, N. Van Doremalen, P. Hudson, H. McCallum, Dose–response and transmission: The nexus between reservoir hosts, environment and recipient hosts. *Philos. Trans. R. Soc. B* **374**, 20190016 (2019).
3. W.-H. W. Lin, R. D. Kouyos, R. J. Adams, B. T. Grenfell, D. E. Griffin, Prolonged persistence of measles virus RNA is characteristic of primary infection dynamics. *Proc. Natl. Acad. Sci. U.S.A.* **109**, 14989–14994 (2012).
4. D. Sissoko, S. Duraffour, R. Kerber, J. S. Kolie, A. H. Beavogui, A.-M. Camara, G. Colin, T. Rieger, L. Oestereich, B. Pályi, S. Wurr, J. Guedj, T. H. T. Nguyen, R. M. Eggo, C. H. Watson, W. J. Edmunds, J. A. Borel, F. R. Koundouno, M. Cabeza-Cabrerizo, L. L. Carter, L. E. Kafetzopoulou, E. Kuisma, J. Michel, L. V. Patrono, N. Y. Rickett, K. Singethan, M. Rudolf, A. Lander, E. Pallasch, S. Bockholt, E. Rodríguez, A. Di Caro, R. Wölfel, M. Gabriel, C. Gurry, P. Formenty, S. Keïta, D. Malvy, M. W. Carroll, X. Anglaret, S. Günther, Persistence and clearance of Ebola virus RNA from seminal fluid of Ebola virus disease survivors: A longitudinal analysis and modelling study. *Lancet Glob. Health* **5**, e80–e88 (2017).
5. J. Bullard, K. Dust, D. Funk, J. E. Strong, D. Alexander, L. Garnett, C. Boodman, A. Bello, A. Hedley, Z. Schiffman, K. Doan, N. Bastien, Y. Li, P. G. Van Caeseele, G. Poliquin, Predicting infectious SARS-CoV-2 from diagnostic samples. *Clin. Infect. Dis.* **71**, 2663–2666 (2020).
6. D. E. Griffin, Why does viral RNA sometimes persist after recovery from acute infections? *PLOS Biol.* **20**, e3001687 (2022).
7. S. R. Compton, L. J. Ball-Goodrich, F. Paturzo, J. D. Macy, Transmission of enterotropic mouse hepatitis virus from immunocompetent and immunodeficient mice. *Comp. Med.* **54**, 29–35 (2004).
8. S. Tovanabutra, V. Robison, J. Wongtrakul, S. Sennum, V. Suriyanon, D. Kingkeow, S. Kawichai, P. Tanan, A. Duerr, K. E. Nelson, Male viral load and heterosexual transmission of HIV-1 subtype E in northern Thailand. *J. Acquir. Immune Defic. Syndr.* **29**, 275–283 (2002).

9. M. J. Matson, E. Ricotta, F. Feldmann, M. Massaquoi, A. Sprecher, R. Giuliani, J. K. Edwards, K. Rosenke, E. de Wit, H. Feldmann, Evaluation of viral load in patients with Ebola virus disease in Liberia: A retrospective observational study. *Lancet Microbe* **3**, e533–e542 (2022).
10. J. A. Hay, L. Kennedy-Shaffer, S. Kanjilal, N. J. Lennon, S. B. Gabriel, M. Lipsitch, M. J. Mina, Estimating epidemiologic dynamics from cross-sectional viral load distributions. *Science* **373**, eabh0635 (2021).
11. E. G. Playford, B. McCall, G. Smith, V. Slinko, G. Allen, I. Smith, F. Moore, C. Taylor, Y.-H. Kung, H. Field, Human Hendra virus encephalitis associated with equine outbreak, Australia, 2008. *Emerg. Infect. Dis.* **16**, 219–223 (2010).
12. P. Eby, A. J. Peel, A. Hoegh, W. Madden, J. R. Giles, P. J. Hudson, R. K. Plowright, Pathogen spillover driven by rapid changes in bat ecology. *Nature* **613**, 340–344 (2023).
13. E. J. Annand, B. A. Horsburgh, K. Xu, P. A. Reid, B. Poole, M. C. de Kantzow, N. Brown, A. Tweedie, M. Michie, J. D. Grewar, Novel Hendra virus variant detected by sentinel surveillance of horses in Australia. *Emerg. Infect. Dis.* **28**, 693–704 (2022).
14. World Health Organization, Prioritizing diseases for research and development in emergency contexts (2022). www.who.int/activities/prioritizing-diseases-for-research-and-development-in-emergency-contexts.
15. H. Field, D. Edson, D. Melville, A. Broos, L. McMichael, N. Kung, C. Smith, D. Jordan, S. Morris, K. Parry-Jones, A. Divljan, R. Davis, P. Kirkland, Spatiotemporal aspects of hendra virus infection in pteropid bats (flying-foxes) in Eastern Australia. *PLOS ONE* **10**, e0144055 (2015).
16. D. J. Becker, P. Eby, W. Madden, A. J. Peel, R. K. Plowright, Ecological conditions predict the intensity of Hendra virus excretion over space and time from bat reservoir hosts. *Ecol. Lett.* **26**, 23–36 (2023).
17. D. J. Páez, J. Giles, H. McCallum, H. Field, D. Jordan, A. J. Peel, R. K. Plowright, Conditions affecting the timing and magnitude of Hendra virus shedding across pteropodid bat populations in Australia. *Epidemiol. Infect.* **145**, 3143–3153 (2017).
18. J. R. Giles, A. J. Peel, K. Wells, R. K. Plowright, H. McCallum, O. Restif, Optimizing noninvasive sampling of a zoonotic bat virus. *Ecol. Evol.* **11**, 12307–12321 (2018).
19. P. Daniels, T. Ksiazek, B. T. Eaton, Laboratory diagnosis of Nipah and Hendra virus infections. *Microbes Infect.* **3**, 289–295 (2001).
20. W. Kermack, A. McKendrick, A contribution to the mathematical theory of epidemics. *Proc. R. Soc. Lond. A* **115**, 700–721 (1927).
21. R. Jaafar, S. Aherfi, N. Wurtz, C. Grimaldier, T. Van Hoang, P. Colson, D. Raoult, B. La Scola, Correlation between 3790 quantitative polymerase chain reaction–positives samples and positive cell cultures, including 1941 severe acute respiratory syndrome coronavirus 2 isolates. *Clin. Infect. Dis.* **72**, e921–e921 (2021).
22. C. E. Snedden, J. O. Lloyd-Smith, Predicting the presence of infectious virus from PCR data: A meta-analysis of SARS-CoV-2 in non-human primates. *PLOS Pathog.* **20**, e1012171 (2024).
23. A. J. Peel, C. K. Yinda, E. J. Annand, A. S. Dale, P. Eby, J.-S. Eden, D. N. Jones, M. K. Kessler, T. J. Lunn, T. Pearson, J. E. Schulz, I. L. Smith, V. J. Munster, R. K. Plowright, Bat One Health Group, Novel Hendra virus variant circulating in black flying foxes and grey-headed flying foxes Australia. *Emerg. Infect. Dis.* **28**, 1043–1047 (2022).
24. M. K. Kessler, D. J. Becker, A. J. Peel, N. V. Justice, T. Lunn, D. E. Crowley, D. N. Jones, P. Eby, C. A. Sánchez, R. K. Plowright, Changing resource landscapes and spillover of henipaviruses. *Ann. N. Y. Acad. Sci.* **1429**, 78–99 (2018).
25. R. K. Plowright, A. J. Peel, D. G. Streicker, A. T. Gilbert, H. McCallum, J. Wood, M. L. Baker, O. Restif, Transmission or within-host dynamics driving pulses of zoonotic viruses in reservoir-host populations. *PLOS Negl. Trop. Dis.* **10**, e0004796 (2016).
26. J. C. Guito, S. G. Kirejczyk, A. J. Schuh, B. R. Amman, T. K. Sealy, J. Graziano, J. R. Spengler, J. R. Harmon, D. M. Wozniak, J. B. Prescott, J. S. Towner, Coordinated inflammatory responses dictate Marburg virus control by reservoir bats. *Nat. Commun.* **15**, 1826 (2024).
27. P. Eby, B. Law, *Ranking the Feeding Habitat of Grey-Headed Flying Foxes for Conservation Management* (Department of Environment, Heritage, Water and the Arts, 2008).
28. V. J. Munster, C. Baas, P. Lexmond, T. M. Bestebroer, J. Guldemeester, W. E. Beyer, E. de Wit, M. Schutten, G. F. Rimmelzwaan, A. D. M. E. Osterhaus, R. A. M. Fouchier, Practical considerations for high-throughput influenza A virus surveillance studies of wild birds by use of molecular diagnostic tests. *J. Clin. Microbiol.* **47**, 666–673 (2009).
29. B. Borremans, C. A. Falvo, D. E. Crowley, A. Hoegh, J. O. Lloyd-Smith, A. J. Peel, O. Restif, M. Ruiz-Aravena, R. K. Plowright, Reconstructing prevalence dynamics of wildlife pathogens from pooled and individual samples. *Peer Commun. J.* **4**, e80 (2024).
30. J. A. Welbergen, J. Meade, H. E. Field, D. Edson, L. McMichael, L. P. Shoo, J. Praszczalek, C. Smith, J. M. Martin, Extreme mobility of the world's largest flying mammals creates key challenges for management and conservation. *BMC Biol.* **18**, 101 (2020).
31. R. C. Team, *R: A Language and Environment for Statistical Computing* (R Foundation for Statistical Computing, 2022).
32. H. Field, C. de Jong, D. Melville, C. Smith, I. Smith, A. Broos, Y. H. N. Kung, A. McLaughlin, Zeddeman, Hendra virus infection dynamics in Australian fruit bats. *PLOS ONE* **6**, e28678 (2011).
33. A. L. Burroughs, P. A. Durr, V. Boyd, K. Graham, J. R. White, S. Todd, J. Barr, I. Smith, G. Baverstock, J. Meers, G. Crameri, L. F. Wang, Hendra virus infection dynamics in the grey-headed flying fox (*Pteropus poliocephalus*) at the Southern-most extent of its range: Further evidence this species does not readily transmit the virus to horses. *PLOS ONE* **11**, e0155252 (2016).
34. A. J. Peel, M. Ruiz-Aravena, K. Kim, B. Scherting, C. A. Falvo, D. E. Crowley, V. J. Munster, E. J. Annand, K. Plain, D. N. Jones-Slobodian, Synchronized seasonal excretion of multiple coronaviruses coincides with high rates of coinfection in immature bats. *Nat. Commun.* **16**, 6579 (2025).
35. B. Linnegar, A. Hoegh, H. McCallum, A. J. Peel, Bridging hosts: Domestic horse density and Hendra virus spillover risk in a changing landscape. *Equine Vet. J.* **58**, 549–563 (2026).
36. T. J. Lunn. "Flying-fox ecology and transmission dynamics of Hendra virus," thesis, Griffith University, Brisbane, Australia (2021).

Acknowledgments: We acknowledge the Kabi Kabi, Turrbal, Widjabul Wia-bal, Yugambeh, and Yuggera Ugarapul people, who are the Traditional Custodians of the land upon which this work was conducted. We would like to thank T. Pearson, D. Karkkainen, T. Padgett-Stewart, J. Scaccia, A. Ananda, E. Glennon, K. Martyn, R. Kirton, H. Eiseman, M. Johnson, K. Yock, E. Skinner, J. Urquhart, R. Muylaert, J. Shabrod, A. Risely, A. Murray, V. Halilovic, L.-a. Lunn, K. Dutton-Registor, K. Winter, M. Walker, G. Smith, C. Pietromonaco, L. Pulscher, C. Sanchez, K. Perry-Jones, C. Parsons, J. Brito, and J. Strazz for assistance in the field. We also thank S. LaTrielle, I. Knights, D. Riseley, and S. Maris Januario da Silva for project support, and the Parks family and other landholders for granting us access to property. This research was conducted under Griffith University Animal Research Authority permits (Certificate: ENV/10/16/AEC and ENV/07/20/AEC), Scientific Purposes Permits from the Queensland Department of Environment and Heritage Protection (WISP17455716 and WA0012532), a permit to Take, Use, Keep or Interfere with Cultural or Natural Resources (Scientific Purpose) from the Department of National Parks, Sport and Racing (WITK18590417), a Scientific License from the New South Wales Parks and Wildlife Service (SL101800), and general and products liability protection permit (GRI 18 GPL), and with permission to undertake research on council and private land. **Funding:** The content of this manuscript does not necessarily reflect the position or the policy of the US government, and no official endorsement should be inferred. The contributions of the NIH authors are considered Works of the United States Government. The findings and conclusions presented in this paper are those of the authors and do not necessarily reflect the views of the NIH or the US Department of Health and Human Services. This work was supported by the following: National Science Foundation DEB1716698 and EF-2231624 (R.K.P., A.J.P., P.E., P.H., J.O.L.-S., H.M., L.P.M., V.J.M., and O.R.); DARPA PREEMPT program Cooperative Agreement no. D18AC00031 (R.K.P., A.J.P., P.E., P.H., J.O.L.-S., H.M., L.P.M., V.J.M., and O.R.); Endeavour Leadership Program Endeavour Postgraduate Leadership Award (T.J.L.); Australian Government Research Training Program scholarship (T.J.L.); Australian Research Council DECRA fellowship DE190100710 (A.J.P.); Queensland Government Accelerate Postdoctoral Research Fellowship (A.J.P.); University of Sydney Horizon Fellowship (A.J.P.); National Institute of Allergy and Infectious Diseases Division of Intramural Research (V.J.M. and C.K.Y.); and US Department of State and the Australian-American Fulbright Commission Fulbright US Student Program (M.K.K.). **Author contributions:** Conceptualization and methodology: T.J.L., B.B., P.E., P.H., D.N.J.-S., M.K.K., J.O.L.-S., H.M., L.P.M., V.J.M., O.R., R.K.P., and A.J.P. Investigation: T.J.L., A.S.D., C.A.F., D.N.J.-S., M.K.K., V.J.M., I.L.S., and C.K.Y. Data curation: T.J.L., D.E.C., C.A.F., D.N.J.-S., M.K.K., M.R.-A., and C.K.Y. Validation: V.J.M., I.L.S., and C.K.Y. Formal analysis: T.J.L., B.B., R.K.P., and A.J.P. Visualization: T.J.L., B.B., R.K.P., and A.J.P. Supervision: P.E., H.M., V.J.M., O.R., R.K.P., and A.J.P. Project administration: T.J.L., A.S.D., D.N.J.-S., M.K.K., H.M., V.J.M., C.K.Y., R.K.P., and A.J.P. Funding acquisition: P.E., P.H., J.O.L.-S., H.M., L.P.M., V.J.M., O.R., R.K.P., and A.J.P. Writing—original draft: T.J.L. Writing—review and editing: all authors. **Competing interests:** The authors declare that they have no competing interests. **Data, code, and materials availability:** All data and code needed to evaluate and reproduce the results in the paper are present in the paper and/or the Supplementary Materials. If not already available as open access files, the datasets generated and analyzed during the current study, and associated code, are available in Zenodo (https://zenodo.org/records/18469713; DOI:10.5281/zenodo.18469713). This study did not generate new materials. The samples analyzed in this study were collected longitudinally under field conditions, and many have been fully consumed during testing; the remaining material is insufficient for distribution. As these are nonrenewable field samples, replication would require collection of comparable specimens using the protocols described in Materials and Methods.

Submitted 5 August 2025
Accepted 1 June 2026
Published 10 July 2026
10.1126/sciadv.aea6654

ScienceAdvances

Periodic shifts in viral load increase risk of Hendra virus spillover from *Pteropus* bats

Tamika J. Lunn, Benny Borremans, Devin N. Jones-Slobodian, Maureen K. Kessler, Adrienne S. Dale, Claude K. Yinda, Manuel Ruiz-Aravena, Caylee A. Falvo, Daniel E. Crowley, James O. Lloyd-Smith, Vincent J. Munster, Peggy Eby, Hamish McCallum, Peter Hudson, Olivier Restif, Liam P. McGuire, Ina L. Smith, Bat One Health Group Collaborators, Raina K. Plowright, and Alison J. Peel

Sci. Adv. **12** (28), eaea6654. DOI: 10.1126/sciadv.aea6654